ISSN: 3071-186X Volume 01, Issue 03, April, 2026

Scienta Press Journals

American Innovator
Journal of Emerging Technologies and Research

Influence of PEO/PMMA polymer electrolyte composition on charge transport and recombination dynamics in dye-sensitized solar cells

S.S. Sharipbaev
Namangan State Technical University, 160115, Namangan, Uzbekistan.
E-mail: sharipbaev1999@gmail.com
ORCID 0009-0009-2269-7711

Abstract

Electrolyte composition plays a decisive role in governing ionic transport, interfacial charge transfer, and recombination dynamics in dye-sensitized solar cells (DSSCs). In this work, a series of polymer-based electrolytes with systematically varied PEO/PMMA ratios were prepared and investigated using electrochemical impedance spectroscopy (EIS) and intensity-modulated photocurrent/photovoltage spectroscopy (IMPS/IMVS). The influence of polymer matrix composition on ionic conductivity, recombination resistance, electron lifetime, diffusion coefficient, and charge collection efficiency was quantitatively evaluated. The results demonstrate that optimized PEO/PMMA ratios can effectively prolong electron lifetime while maintaining sufficient ionic conductivity. The findings provide a direct electrochemical basis for electrolyte engineering in advanced DSSCs.

Keywords: Dye-sensitized solar cells; Polymer electrolyte; PEO/PMMA; Electrochemical impedance spectroscopy; IMPS/IMVS; Electron lifetime; Recombination resistance

PACS: 82.45.Yz, 88.40.jr, 73.50.Pz, 82.47.Aa

1. Introduction

Dye-sensitized solar cells (DSSCs) have attracted sustained interest as a cost-effective photovoltaic technology with favorable performance under diffuse illumination conditions [1,2]. A typical DSSC comprises a nanostructured TiO_2 photoanode sensitized with molecular dyes, a redox electrolyte mediating charge regeneration, and a platinum counter electrode (Figure 1). The photoelectrochemical processes at the semiconductor–electrolyte interface determine the overall photovoltaic performance [3,4].

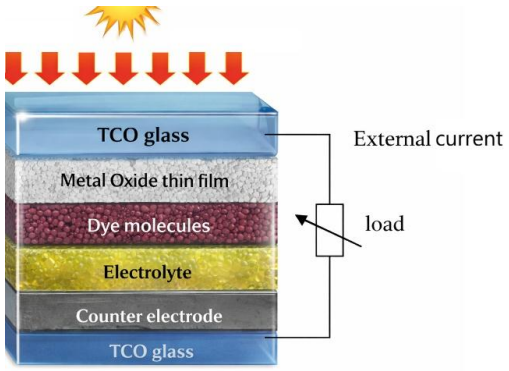

Figure 1. Schematic structure of a DSSC device.

While the TiO_2 photoanode governs electron transport, the electrolyte controls ionic diffusion and critically influences recombination dynamics at the TiO_2/dye/electrolyte interface. Conventional liquid iodide/triiodide electrolytes provide high ionic conductivity but suffer from volatility and long-term stability issues [5,6]. Polymer-modified and gel-type electrolytes based on polyethylene oxide (PEO) and poly(methyl methacrylate) (PMMA) have emerged as promising alternatives, offering improved mechanical stability while maintaining efficient charge transport [7,8].

The balance between polymer flexibility and segmental mobility is critical for facilitating I^-/I_3^- diffusion while suppressing charge recombination. Modern studies demonstrate that PEO provides high segmental chain mobility favorable for ionic transport, while PMMA contributes to mechanical stability and improved interfacial passivation at the TiO_2 surface. The optimization of their ratio offers a practical route to tailoring electrolyte properties for specific photoanode architectures [7,8].

Electrochemical impedance spectroscopy (EIS) and intensity-modulated spectroscopy techniques (IMPS/IMVS) provide powerful diagnostic tools for probing charge transport, recombination, and

interfacial processes in DSSCs. These techniques enable quantitative extraction of key physical parameters such as electron lifetime, recombination resistance, diffusion coefficient, and electron diffusion length [9–11]. In this study, the influence of PEO/PMMA ratio on charge transport and recombination dynamics is systematically investigated using these complementary electrochemical methods.

2. Materials and Methods

2.1. Preparation of polymer electrolytes

A series of seven polymer-based electrolytes was prepared by systematically varying the PEO/PMMA mass ratio while keeping the concentrations of DMF (1 ml), EC (0.25 ml), PC (0.25 g), TPAI (0.2 g), and I_2 (0.02 g) constant (Table 1). Each component was dissolved sequentially and stirred for 30 minutes using a Stuart SB 162-3 hotplate magnetic stirrer. TPAI was added and the mixture was stirred at 70°C until homogeneous. After cooling, I_2 was added (10% of TPAI mass) and mixed using an IKA C-MAG apparatus, then stored in darkness for 24 hours [7,11].

Table 1. Composition of polymer-based electrolytes

No.	PEO (g)	PMMA (g)	DMF (ml)	EC (ml)	PC (g)	TPAI (g)	I_2 (g)
1	1.0	0	1	0.25	0.25	0.2	0.02
2	0.8	0.2	1	0.25	0.25	0.2	0.02
3	0.6	0.4	1	0.25	0.25	0.2	0.02
4	0.5	0.5	1	0.25	0.25	0.2	0.02
5	0.4	0.6	1	0.25	0.25	0.2	0.02
6	0.2	0.8	1	0.25	0.25	0.2	0.02
7	0	1.0	1	0.25	0.25	0.2	0.02

2.2. DSSC fabrication

Single-layer TiO_2 photoanodes were fabricated by spin-coating TiO_2 paste (P25) onto FTO glass substrates at 3000 rpm, followed by annealing at 450°C for 30 minutes. The photoanodes were sensitized in 0.3 mM ruthenium-based dye solution (ethanol:acetonitrile 1:1) at 40°C for 24

hours. The working principle of the n-type semiconductor solar cell is illustrated in Figure 2 [3,4].

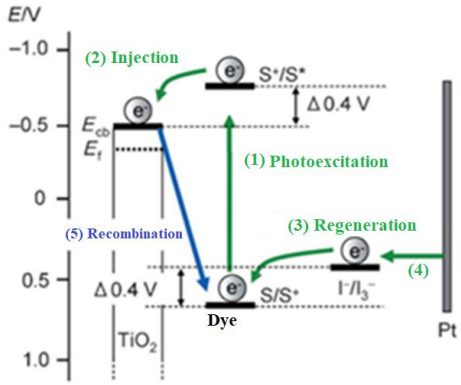

Figure 2. Working principle of n-type semiconductor DSSCs and their physical processes.

2.3. Electrochemical characterization

Ionic conductivity was analyzed using a HIOKI 3531 Z Hi-Tester via EIS at an alternating voltage of 10 mV in the frequency range 50 Hz to 100 kHz. The impedance consists of real and imaginary parts [11]:

$$Zr = R + \cos(\pi p/2) / (k^{-1}\omega^{p}) \quad \text{and} \quad Zi = \sin(\pi p/2) / (k^{-1}\omega^{p})$$

where Zr and Zi are the real and imaginary impedance components, ω is the frequency, and p = 2tgα/π. The ionic conductivity is calculated as σ = l/(R·S), where l is the electrolyte thickness, R is the active resistance, and S is the surface area [11,12].

2.4. IMPS/IMVS measurements

Intensity-modulated photocurrent spectroscopy (IMPS) and intensity-modulated photovoltage spectroscopy (IMVS) were performed to determine electron transport time (τtr) and electron lifetime (τrec). From these parameters, the charge collection efficiency ηcoll = 1 − τtr/τrec, electron diffusion coefficient D = d²/(2.35τtr), and electron diffusion length Ln = √(D·τrec) were calculated [9,10].

3. Results and Discussion

3.1. EIS Nyquist plot analysis

Figure 3 shows a representative Nyquist plot obtained from electrochemical impedance spectroscopy of one of the polymer electrolyte samples. The plot displays a characteristic semicircular arc in the mid-frequency region, corresponding to the recombination resistance

at the TiO_2/dye/electrolyte interface. The intercept with the real axis at high frequency represents the bulk resistance R of the electrolyte. The parameter p is determined from the angle of the low-frequency tail using p = 2tgα/π. The real part of the impedance equals the active resistance (Zr = R), which is directly extracted from the Nyquist plot [7,11].

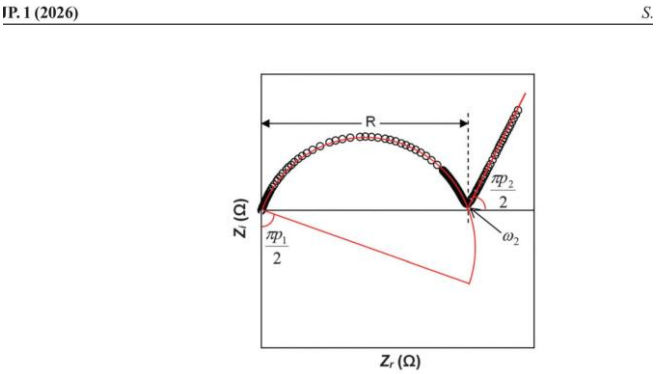

Figure 2. Electrochemical impedance spectroscopy (EIS) graph of an electrolyte [11]

Figure 3. Electrochemical impedance spectroscopy (EIS) Nyquist plot of a polymer electrolyte sample.

3.2. Impedance spectroscopy analysis

EIS measurements were performed under dark conditions at open-circuit voltage. The impedance spectra were analyzed using equivalent circuit models commonly adopted for DSSC analysis. In Nyquist plots, the mid-frequency semicircle is associated with recombination resistance at the TiO_2/dye/electrolyte interface, while low-frequency features relate to ionic diffusion within the electrolyte. The electron lifetime was determined from the Bode phase plots using τe = 1/(2πfmax), where fmax is the characteristic frequency of the maximum phase shift. Additionally, the recombination dynamics were evaluated using τe = Rrec · Cμ, where Rrec is the recombination resistance and Cμ is the chemical capacitance. These expressions allow direct quantitative comparison of charge recombination processes for different electrolyte compositions [11,12].

The electrical capacitance of the electrolyte is determined by $C = k^{-1} = \varepsilon_r\varepsilon_0 S/d$, where εr is the relative permittivity, ε0 is the electric constant, S is the contact area, and d is the electrolyte layer thickness. The ionic conductivity is calculated as σ = l/(R·S), where l is the electrolyte thickness and R is the active resistance determined from the real axis intercept of the Nyquist plot [7,11].

Systematic variation of the PEO/PMMA ratio significantly influenced the impedance characteristics. Higher PEO content generally increased ionic conductivity due to enhanced segmental chain mobility, facilitating iodide/triiodide diffusion within the polymer matrix. Conversely, increasing PMMA content improved interfacial passivation at the TiO_2 surface by forming a more rigid polymer network that reduces back-electron transfer to triiodide species, leading to higher recombination resistance [7,8].

3.3. IMPS/IMVS analysis

The IMPS and IMVS spectra obtained from the experiments are shown in Figures 4 and 5. Both plots exhibit characteristic maxima from which the electron transport time and electron lifetime were extracted. These parameters enable calculation of charge collection efficiency, diffusion coefficient, and diffusion length [9,10].

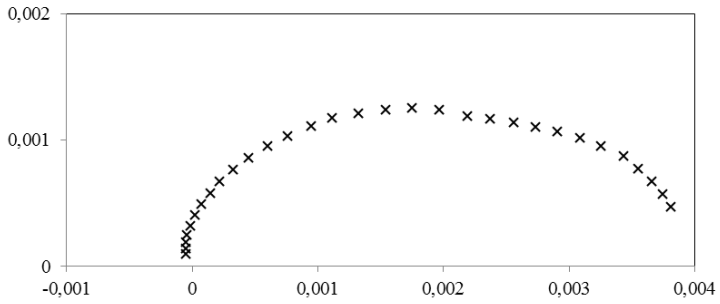

Figure 4. Intensity-modulated photocurrent spectroscopy (IMPS) spectrum.

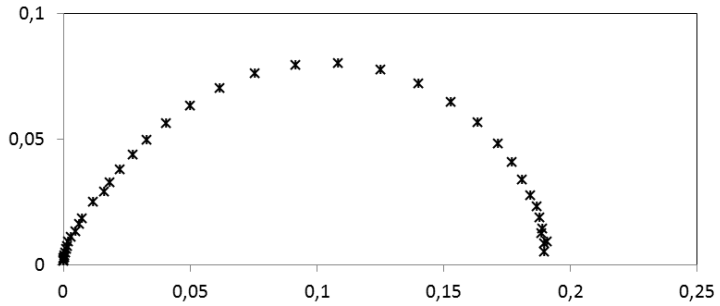

Figure 5. Intensity-modulated photovoltage spectroscopy (IMVS) spectrum.

3.4. Effect of PEO/PMMA ratio on electron lifetime and recombination

Comparative analysis reveals that electrolyte composition significantly affects recombination dynamics. Pure PEO-based electrolytes (sample 1)

exhibited the highest ionic conductivity but moderate recombination resistance due to insufficient surface passivation. Conversely, pure PMMA-based electrolytes (sample 7) demonstrated high recombination resistance but reduced ionic mobility. Intermediate compositions (samples 3–5) provided the optimal balance between ionic transport and interfacial passivation, yielding prolonged electron lifetime without severely compromising conductivity [7,8,11].

The electron diffusion length Ln must exceed the photoanode thickness d for efficient charge collection (Ln > d). For the investigated single-layer photoanodes (55–58 μm), the optimized electrolyte compositions satisfy this criterion, confirming that the PEO/PMMA ratio can be tuned to achieve efficient charge collection in thick photoanode configurations [9,10].

3.5. Single-layer vs. bilayer: electrolyte-dependent behavior

Electrolyte composition affects single-layer and bilayer DSSCs differently. In single-layer photoanodes, polymer content primarily influences ionic transport resistance and interfacial recombination. Bilayer photoanodes exhibit enhanced sensitivity to electrolyte composition due to the compact underlayer modifying the electric field distribution. Polymer-modified electrolytes can synergistically interact with multilayer architectures, leading to increased recombination resistance [12,13]. The results indicate that electrolyte optimization is particularly critical for thick and multilayer DSSC configurations.

4. Conclusions

A systematic investigation of PEO/PMMA polymer electrolyte composition on charge transport and recombination dynamics in DSSCs was performed using EIS and IMPS/IMVS techniques. The results demonstrate that the PEO/PMMA ratio critically governs the balance between ionic conductivity and interfacial passivation at the TiO_2/dye/electrolyte interface. Pure PEO-based electrolytes exhibited the highest ionic conductivity but moderate recombination resistance, while pure PMMA-based systems showed the opposite trend.

Optimized intermediate PEO/PMMA compositions provide prolonged electron lifetime and enhanced recombination resistance while maintaining adequate ionic conductivity for efficient charge regeneration. The IMPS/IMVS analysis confirmed that optimized electrolyte

compositions satisfy the condition Ln > d for efficient charge collection in photoanodes with thicknesses of 55–58 μm.

The effectiveness of electrolyte optimization is strongly coupled to photoanode architecture, with bilayer DSSCs exhibiting greater sensitivity to polymer composition due to modified electric field distribution at the compact underlayer. These findings provide a direct electrochemical basis for integrated electrolyte–photoanode optimization strategies in advanced DSSCs, supporting the development of stable and efficient devices for practical applications including building-integrated photovoltaics and indoor energy harvesting.

References

1. O'Regan B., Grätzel M. A low-cost, high-efficiency solar cell based on dye-sensitized colloidal TiO_2 films. Nature, 353 (1991) 737–740.
2. Grätzel M. Dye-sensitized solar cells. J. Photochem. Photobiol. C, 4 (2003) 145–153.
3. Zhang Q., Cao G. Nanostructured photoelectrodes for DSSCs. Nano Today, 6 (2011) 91–109.
4. Bisquert J. Theory of the impedance of electron diffusion and recombination in a thin layer. Phys. Chem. Chem. Phys., 5 (2003) 5360–5364.
5. Park N.-G. Toward stable dye-sensitized solar cells. J. Phys. Chem. Lett., 4 (2013) 2423–2429.
6. Bella F., Gerbaldi C. et al. Polymeric electrolytes for DSSCs. J. Power Sources, 310 (2016) 116–123.
7. Arof A.K., Amirudin S., Yusof S.Z., Noor I.M. A method based on impedance spectroscopy to determine transport properties of polymer electrolytes. Phys. Chem. Chem. Phys., 16 (2014) 1856–1867.
8. Aram E., Ehsani M., Khonakdar H.A. Improvement of ionic conductivity of quasi-solid-state DSSC using PEO/PMMA gel electrolyte. Thermochimica Acta, 615 (2015) 61–67.
9. Freitag M. et al. DSSCs for efficient power generation under ambient lighting. Nature Photonics, 11 (2017) 372–378.
10. Fabregat-Santiago F., Bisquert J. et al. Influence of electrolyte on transport and recombination in DSSCs. J. Phys. Chem. C, 111 (2007) 6550–6560.

11. Mamatkarimov O.O., Uktamaliyev B., Abdukarimov A.A. Determination of ionic conductivity of polymer electrolytes using EIS. An International Multidisciplinary Research Journal, 11(7) (2021) 141–146.
12. Abdukarimov A.A. et al. Characteristics of DSSCs using liquid and gel polymer electrolytes with tetrapropylammonium salt. Opt. Quantum Electron., 52 (2020) 1–15.
13. S.S. Sharipbaev, O.O. Mamatkarimov, N.Yu. Sharibaev, A.A. Abdukarimov, A.K. Arof, East Eur. J. Phys. 1, 373 (2026)